

Supporting Information

Mn(III)-mediated carbon-centered radicals generate an enhanced immunotherapeutic effect

Jiaxuan Li,^{+[a]} Baifei Hu,^{+[b]} Zelong Chen,^{+[a]} Jiahui Li,^[a] Wenjuan Jin,^[a] Yi Wang,^[a]
Yichen Wan,^[a] Yinghua Lv,^[a] Yuxin Pei,^{*[a]} Hongtao Liu,^{*[b]} Zhichao Pei^{*[a]}

^aCollege of Chemistry & Pharmacy

Northwest A&F University

Yangling, Shaanxi 712100, P. R. China.

E-mail: peiyx@nwafu.edu.cn; peizc@nwafu.edu.cn

Fax: +86-29-8709-1196

^bCollege of Basic Medical Sciences

Hubei University of Chinese Medicine

Huangjiahu West Road 16, Wuhan 430065, PR China.

E-mail: hongtaoliu@hbtcn.edu.cn

*These authors contributed equally to this work.

Contents

General information.....	3
Figure S1 - Figure S5.....	10
Synthesis and characterization of the compounds.....	13
Figure S23 - Figure S34.....	27
References	34

General information

Experimental Procedures

Materials: Hydrochloric acid (HCl) and aqueous ammonia ($\text{NH}_3 \cdot \text{H}_2\text{O}$) were purchased from Xilong Chemical Co., Ltd (Guangdong, China). Sodium hydroxide (NaOH) and 30% H_2O_2 solution were obtained from Guanghua Sci-Tech Co., Ltd (Guangdong, China). Sodium methoxide (MeONa), lactose, boron trifluoride etherate and hydroquinone were gotten from Aladdin Biochemical Technology Co., Ltd (Shanghai, China). Tetrabutylammonium bromide (TBAB), 1,3-diphenylisobenzofuran (DPBF), cinnamic aldehyde (CA), lactobionic acid (LBA) and methylene blue (MB) purchased from Energy Chemical Reagent Co., Ltd (Anhui, China). Tetraethyl orthosilicate (TEOS), 1,2-dibromoethane, isoniazid (INH) and manganese(III) acetate dihydrate were gotten from Macklin Chemical Reagent Co., Ltd (Shanghai, China). Manganese(II) chloride tetrahydrate purchased from adamas-beta (Shanghai, China). Sodium azide was purchased from Amresco (USA). 2-[2-(2-chloroethoxy) ethoxy] ethanol was obtained from Heowns Company (Tianjin, China). Palladium 5% on carbon (Pd/C) was purchased from Kaida Chemical Co., Ltd (Shaanxi, China). Chloroform, pyridine, acetic anhydride, potassium permanganate (KMnO_4), potassium iodide (KI) and N, N-dimethylformamide (DMF) were from Kelong Chemical Reagent Factory (Chengdu, China). Iodine and ferric chloride (FeCl_3) were from Bodi Chemical Co., Ltd (Tianjin, China). Sodium carbonate (Na_2CO_3) was obtained from Zhiyuan Chemical Reagent Co., Ltd (Tianjin, China). Sodium thiosulfate standard solution was purchased from Yida Technology (Quanzhou, China). Sodium thiosulfate was from Tianli Chemical Reagent Co., Ltd (Tianjin, China). Methyl thiazolyl tetrazolium (MTT) was purchased from Xiya Reagent Company (Chengdu, China). Reduced glutathione (GSH) assay kit, Hoechst 33258, 2',7'-dichlorofluorescein diacetate (DCFH-DA) and anti-CALR polyclonal antibody were obtained from solarbio science & technology Co., Ltd (Beijing, China). DAPI was from Leagene biotechnology (Beijing, China). RPMI media 1640 was obtained from Gibco BRL company (MD, USA). Fetal bovine serum (FBS) was gotten from Yuanheng Jinma Biotechnology Company (Beijing, China). Streptomycin and penicillin were from KeyGEN BioTECH Co., Ltd (Nanjing, China). Paraformaldehyde solution (4% PFA) and chlorine e6 (Ce6) was from Yuanye Bio-Technology Co., Ltd (Shanghai, China). Hypoxyprobe Plus Kit was from Hypoxyprobe, Inc. (USA). ATP assay kit, Alexa Fluor 488-labeled goat anti-rabbit and Alexa Fluor 647-labeled goat anti-rabbit were purchased from Beyotime Biotechnology (Shanghai, China). HMGB-1 and IL-6 ELISA kits were from Meibiao Biotechnology Co., Ltd (Jiangsu, China). Anti-mouse CD3, APC, anti-mouse CD8, PE and regulatory T cell detection kit were purchased from Multi sciences (Hangzhou, China). NOS2 polyclonal antibody and CD206 polyclonal antibody was from ImmunoWay Biotechnology (USA). All reagents were used without further purification. Human liver hepatocellular carcinoma

HepG2, human cervical cancer HeLa, human liver HL7702 cell lines were obtained from KeyGEN BioTECH Co., Ltd (Nanjing, China).

Instrumentation: AUW120D Analytical Balances (Shimadzu, Japan). PB-10 pH meter (Sartorius, Germany). ^1H NMR spectra (500 MHz or 400 MHz) and ^{13}C NMR spectra (125 MHz or 100 MHz) were recorded on Bruker Spectrometer (Bruker, Germany) and are calibrated relative to residual solvent signals¹. DLS and zeta potential measurements were performed on Malvern Zen3600 instrument (Malvern, UK). UV-vis spectra were recorded with Shimadzu 1750 UV-visible spectrophotometer (Japan) at 25 °C. Transmission electron microscopy FEI Tecnai F20 (USA) or HITACHI HT7800 (Japan). XPS spectra were recorded with Thermo Scientific K-Alpha (USA). HRMS were recorded with AB SCIEX LC-30A+TripleTOF5600+ (USA). Confocal laser scanning microscope Lecia Stellaris 8 (Germany). Flow cytometry analysis is performed on the BD FACSAria III (USA).

Experimental Section

Preparation of sSiO₂ nanoparticles: 5 mL TEOS was added dropwise to a mixed solution consisting of 140 mL of ethanol, 20 mL of RO water and 5 mL of aqueous ammonia at 45 °C, and stir for 3 h. After the reaction was completed, the sSiO₂ was collected by centrifugation (12000 r/min, 10 min), washed with ethanol three times, and dried in vacuum.

Preparation of sSiO₂@MnO₂ nanoparticles: A suspension of sSiO₂ (40 mg, 10 mL) was added dropwise to aqueous solution of KMnO₄ (300 mg, 10 mL) and sonicated for 6 h to synthesize MnO₂ coated sSiO₂ (sSiO₂@MnO₂). The nanoparticles were collected by centrifugation (10000 r/min, 10 min) and washed three times with water.

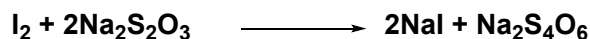
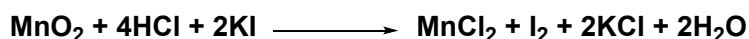
Preparation of HMnO₂ nanoparticles: sSiO₂@MnO₂ was dispersed into 2 M Na₂CO₃ aqueous solution at 60 °C and stirred for 12 h after that HMnO₂ was collected by centrifugation. The obtained HMnO₂ water was washed several times, and finally dispersed in water and stored at 2-8 °C.

Preparation of MPL nanoparticles: 10 mL HMnO₂ (2 mg/mL) solution was mixed with 10 mL AMP6 β LacPy (2 mg/mL) solution. After stirred for 12 h, the MPL was collected by centrifugation (10000 r/min, 10 min).

INH-CA and Ce6 loading: the MPL solution (1 mg/mL) was mixed with Ce6 (1.1 mg/mL) and INH-CA (1.1 mg/mL) and stirred for 12 h. Ce6 and INH-CA were co-loaded into MPL yielding MPL@ICC which was used for further experiments.

The content of MnO₂ in MPL was determined by titration: Dried MPL (200 mg), KI (1 g) and 50 mL of RO water were added into a conical flask, 6 M HCl (10 mL) was added after KI was completely dissolved and then shake until the MPL was completely dissolved. Quickly titrate with 0.1006 M Na₂S₂O₃ solution until the solution in conical flask was pale yellow, added 3 mL of 0.5% starch solution

and continue to titrate until the blue color disappeared. The reaction is as follows:



Drug release studies: To study the Ce6 and INH-CA release, a solution of MPL@ICC (1 mg/mL) was dialyzed against PBS with different conditions (7.4, 5.8 and 5.8 + 10 mM GSH) under room temperature. The amounts of Ce6 and INH-CA release at different time points were measured by UV-vis spectra.

Degradation of H₂O₂ produces oxygen: 200 mL H₂O₂ solution (100 μM) was sealed with liquid paraffin, and then different concentrations of HMnO₂ nanoparticles were added. The dissolved oxygen concentration changes in H₂O₂ solutions were measured with an oxygen probe (JPBJ-608, Shanghai REX Instrument Factory).

GSH consumption detection: 0.1 mL GSH solution (0.8 mg/mL) was mixed with 0.1 mL of MPL solution at different concentrations for 15 min, and then use the GSH detection kit (Solarbio Science & Technology Co., Ltd) to detect the consumption of GSH.

Free radical generation: The ESR study used the spin trapping agent 100 mM DMPO, 8 mM H₂O₂, 8 mM INH and 2 mM HMnO₂. 1 mL 3.6 mg/mL MnO₂ aqueous solution was mixed with 1 mL 5.4 mg/mL INH aqueous solution, react at 37 °C for 24 h, and then the reaction solution was collected by centrifugation (10000 r/min, 10 min). The supernatant was freeze-dried and characterized by HRMS. The precipitate was vacuum dried and subjected to XPS detection. PBS buffer solution containing 10 μg/mL MB, 8 mM H₂O₂, 8 mM INH and 2 mM HMnO₂ was allowed to stand at 37 °C for 24 h. The MB degradation was monitored by the UV-vis absorption spectra. For Mn(II)Cl₂, Mn(III)(OAc)₃ and MnOx, 2 mM HMnO₂ were changed to equal molar amounts of Mn(II)Cl₂·4H₂O, Mn(III)(OAc)₃·2H₂O, and the above precipitates obtain from MnO₂ reacts with INH in an aqueous solution (assuming that the component of the precipitate is MnO_{1.5}), other operations are the same.

Photostability analysis of Ce6 and MPL@ICC: The aqueous solution of Ce6 and MPL@ICC (Ce6 concentration is 50 ug/mL) was irradiated under 660 nm light (7 mW/cm²). The absorbance change of characteristic absorption peak (Ce6: 641 nm and MPL@ICC: 681 nm) was measured using a UV-visible spectrophotometer at 0, 5, 10, 15, 20, 25, 30 min.

Singlet oxygen generation ability analysis: DPBF was used to detect the ¹O₂ generation ability of MPL@ICC under continuous irradiation. DPBF and Ce6 + DPBF groups were set as controls. MPL@ICC and DPBF were quickly mixed under dark conditions to obtain a mixed solution of MPL@ICC (Ce6 dose of 2 μg/mL) and DPBF (30 μg/mL). Afterwards, the mixed solution was exposed to

irradiation of light (660 nm, 5 mW/cm²). The absorbance change of DPBF at a wavelength of 412 nm was detected by using UV-vis spectrophotometer.

In vitro cell experiments: The four cells lines, HL7702, HepG2, H22, and HeLa used in the experiment were all cultured in RPMI-1640 medium containing 10% FBS, 1% penicillin-streptomycin mixture. All cells were incubated at 37 °C in a 5% CO₂ atmosphere unless otherwise stated.

Intracellular uptake of MPL@ICC or HMnO₂@INH-CA/Ce6: HepG2, HL7702, H22 and HeLa cells were cultured in 35 mm cell culture dish (1 × 10⁵ per dish) in the dark for 24 h. Then the cells were incubated with MPL@ICC or HMnO₂@INH-CA/Ce6 (30 µg/mL) for another 3 h. For LBA block, cells were transferred to fresh medium containing 4 mM LBA for 6 h in advance to block. After fixed by 4% paraformaldehyde solution (Yuanye Bio-Technology Co., Ltd), nuclei were stained with Hoechst 33258 (Solarbio Science & Technology Co., Ltd). The fluorescence of Ce6 (Ex/Em: 660/710 nm) was observed by confocal laser scanning microscope (CLSM). Cells were washed three times with PBS between each step.

Intracellular hypoxia detection: HepG2 cells were cultured in 35 mm cell culture dish (1 × 10⁵ per dish) for 24 h in the incubator. Except for the normoxia group, the rest of all groups were sealed with liquid paraffin. The hypoxia group was not further treated, while INH-CA (9 µg/mL), Ce6 (28 µM), MPL and MPL@ICC (dose of MPL = 25 µg/mL) were added to different groups, respectively. Hypoxyprobe Plus Kit (Hypoxyprobe, Inc.) was used to detect hypoxia levels after 3 h of cell culture according to the manufacturer's instructions. Hoechst 33258 was used for nuclear staining and the fluorescence was observed by CLSM.

Intracellular GSH depletion: HepG2 cells were cultured in 6-well plate for 24 h before the cells were transferred to fresh medium containing MPL (25 µg/mL) to continue culturing for 4, 8, 12 h. After that the cells were collected to detect the Intracellular GSH content according to the operation of the GSH detection kit (Solarbio Science & Technology Co., Ltd).

Intracellular oxidative stress detection: Intracellular oxidative stress detection was performed following the indicator's instructions. Briefly, H22 cells were cultured in 6-well plates (1 × 10⁵ per well) and treated with PBS, MPL, MPL@IC, MPL@Ce6, MPL@ICC (INH-CA = 9 µg/mL, Ce6 = 28 µM, MPL = 25 µg/mL) for 12 h. After treated with or without 660 nm light irradiation (5 mW/cm², 5 min), the cells were stained with DCFH-DA (10 µM, Solarbio Science & Technology Co., Ltd) for 30 min. Finally, cells were imaged by a CLSM. Cells were washed three times with 1640 medium between each step.

Biocompatibility assay: HL7702 cells were seeded into 96-well plates (5 × 10³ per well) until adherent and then incubated with different concentrations of MPL

or MPL@ICC for 24h. The standard thiazolyl tetrazolium (MTT) test was applied to measure the cell viabilities relative to untreated cells.

For in vitro combination therapy: HepG2 cells were seeded into 96-well plates (5×10^3 per well) and cultured for 24 h. After cells adherent, they were incubated with different conditions for 4 h and then were transferred into fresh media after washing three times with PBS. After treated with or without 660 nm light irradiation (5 mW/cm^2 , 30 min), the cells were incubated for another 24 h before the MTT assay to measure relative cell viabilities.

CRT expression, ATP, and HMGB-1 release: To evaluate the ICD after MPL@ICC + Light treatment, CRT exposure in the surface of H22 tumor cells was determined by immunofluorescence staining. After 3 h incubation with PBS, MPL, MPL@IC, free Ce6, MPL@Ce6 or MPL@ICC (dose of INH-CA = $9 \mu\text{g/mL}$, Ce6 = $28 \mu\text{M}$, MPL = $25 \mu\text{g/mL}$), cells in the light group were irradiated with 660 nm-light (2 mW/cm^2) for 3 min. Cells were collected by centrifugation after an additional 3 h or 24 h of incubation and washed twice with PBS before making cell smears. Meanwhile, the culture medium was carefully collected into tube for the determination of HMGB-1. The cell was treated with anti-CALR primary antibody (dilution 1:200, Solarbio Science & Technology Co., Ltd) and Alexa Fluor 488-labeled goat anti-rabbit secondary antibody (dilution 1:500, Beyotime). Hoechst 33258 was used for nuclear staining and the fluorescence was observed by CLSM. The HMGB-1 were determined by a HMGB-1 ELISA kits (Meibiao Biotechnology Co., Ltd) according to the manufacture's protocol. For ATP detection, cells were incubated with PBS, MPL, MPL@IC, free Ce6, MPL@Ce6 or MPL@ICC (dose of INH-CA = $9 \mu\text{g/mL}$, Ce6 = $28 \mu\text{M}$, MPL = $25 \mu\text{g/mL}$) for 8 h. Then light exposure and continued 3 h incubation was performed on ice. The extracellular ATP was determined on a luminometer (GloMax 20/20) using an ATP assay kit (Beyotime) according to the manufacturer's protocol.

Animal models: Female Balb/c mice (6-8 weeks) were purchased from Xian Yi Fengda Biological Technology Co., Ltd, and all animal procedures complied with all relevant ethical regulations and were approved by the Northwest A&F University Animal Care Committee (NWAFU-314020038). H22 cells (5×10^5) suspended in $100 \mu\text{L}$ of PBS were subcutaneously injected into the back of mouse. The mice bearing H22 tumors were treated when the volume of tumor reached about $100\sim 200 \text{ mm}^3$. The volume of tumors was calculated according to the formula: $\text{volume} = (\text{width}^2 \times \text{length})/2$.

For tumor cells rechallenge: After 3 h incubation with MPL@ICC, H22 tumor cells were irradiated with 660 nm-light (2 mW/cm^2) for 3 min. Cells were collected by centrifugation and 3×10^5 cells were injected into the right hind limb of mice. After 7 days, 1×10^5 untreated H22 cells were injected into the mouse left hindlimb and the survival time of the mice was recorded (the mice were considered dead when the tumor volume exceeded 2000 mm^3).

In vivo imaging: After the tumors reached 200 mm³, MPL@ICC (100 µL, dose of Ce6 78 µg/mL) were intravenously injected. The fluorescent imaging was performed using a vivo imaging system (IVIS Lumina II, PerkinElmer) at predetermined time (0, 2, 4, 6, 12, 24, 36, 48 h). At the end of experiment, tumors and major organs were obtained for fluorescence imaging (Ce6, Ex/Em: 675 nm/Cy 5.5). The semiquantitative biodistribution analysis was calculated via fluorescence.

In vivo tumor hypoxia detection: H22 tumor-bearing mice were injected with PBS, free drugs and MPL@ICC by tail vein 12 h in advance. Tumors were surgically excised 90 min after intraperitoneal injection with pimonidazole hydrochloride (60 mg/kg) (Hypoxyprobe Inc.). Tumor tissue was frozen in liquid nitrogen and then embedded with OCT (Sakura, Japan) and sectioned. For detection of pimonidazole, the tumor sections were treated with FITC-conjugated anti-pimonidazole primary antibody (dilution 1:200, Hypoxyprobe Inc.). Cell nuclei were stained with DAPI (dilution 1:5000, Leagene biotechnology). The obtained slices were observed by CLSM.

In vivo tumor pH detection: H22 tumor-bearing mice were injected with PBS, MPL and MPL@ICC by tail vein 24 h in advance. Then tumors were surgically excised and cut into small pieces, added to water (1:10, w:w) and quickly homogenized for pH detection with a pH meter.

In vivo anti-tumor therapy: When the tumor reached approximately 100~200 mm³, H22 bearing mice were randomly divided into seven groups: PBS, MPL, free drugs + Light, MPL@IC, MPL@ICC, MPL@Ce6 + Light, MPL@ICC + Light. (MnO₂ = 9 mg/kg, Ce6 = 7.8 mg/kg, and INH-CA = 4.1 mg/kg). 660 nm light irradiation (0.4 W/cm²) was applied at the tumor site for 5 min after 12 h injection. The volume of tumors and mice body weight were monitored every 2 days for 2 weeks (The scar size was continued to be measured if the tumor disappears). At the end of treatments, mice were sacrificed by cervical dislocation under deep anesthesia. The tumors were weighed and stained with H&E and TUNEL by standard protocols to evaluate the therapeutic efficacy. Major organs were harvested, and H&E staining was performed to assess biosafety.

Immunological effects of combination treatment: H22 tumor-bearing mice were randomly divided into 7 groups and i.v. injected with 100 µL of PBS, MPL, free drugs + Light, MPL@IC, MPL@ICC, MPL@Ce6 + Light, MPL@ICC + Light. (MnO₂ = 9 mg/kg, Ce6 = 7.8 mg/kg, and INH-CA = 4.1 mg/kg). The 660-nm light irradiation was conducted at 12 h (0.4 W/cm², 5 min) post injection. At day 5 post irradiation, mice were sacrificed and blood was collected to determine IL-6 using ELISA assay (Meibiao Biotechnology Co., Ltd), and tumor tissues were collected for INF-γ and TNF-α detection by RT-PCR. For flow cytometry, tumor tissues were cut into small pieces and put into a glass homogenizer containing PBS solution (pH = 7.4 and 1% FBS was added). Single cell suspension was

prepared by gentle pressure trituration with the homogenizer without addition of digestive enzyme. Afterward, cells were stained with fluorescence-labeled antibodies according to the manufacturer's protocol before the removal of red blood cells (RBC) using the RBC lysis buffer. For regulatory T cells (Treg) evaluation, cells were stained with anti-mouse CD4, FITC, anti-mouse CD25, APC, and anti-mouse FoxP3, PE (Multi sciences) antibodies. Meanwhile, cells were stained with anti-mouse CD3, APC and anti-mouse CD8, PE (Multi sciences) for evaluating cytotoxic T lymphocytes (CTL) infiltration. CD4⁺CD25⁺FoxP3⁺ and CD3⁺CD8⁺ cells were defined as Treg and CTL, respectively.

M1/M2 macrophage detection: the tumors were fixed by using Bouin's fixative before were made into paraffin sections. Sections were dewaxed with xylene and boiled with citrate-EDTA antigen retrieval solution (Beyotime) then labeled with antibodies. NOS2 polyclonal antibody (dilution 1:200, ImmunoWay Biotechnology) and Alex 488-conjugated anti-rabbit secondary antibody (dilution 1:500, Beyotime) was used to label M1 macrophages. CD206 polyclonal antibody (dilution 1:200, ImmunoWay Biotechnology) and Alex 647-conjugated anti-rabbit secondary antibody (dilution 1:500, Beyotime) was used to label M2 macrophages.

Statistical analysis: All of the data were presented as the mean \pm SD. from a minimum of three independent experiments. Data analysis was performed using Microsoft Excel version LTSC 2021, Image J (version 1.53c), and OriginPro Learning Edition (2023b). Statistical parameters including statistical analysis, statistical significance, and n value were indicated in the figure legends. For statistical comparison, we performed two-tailed Student's t-test, Mantel-Cox test. A value of $p < 0.05$ was considered significant, different significance levels are indicated as * $p < 0.05$, ** $p < 0.01$, *** $p < 0.001$, or not significant (n.s.)

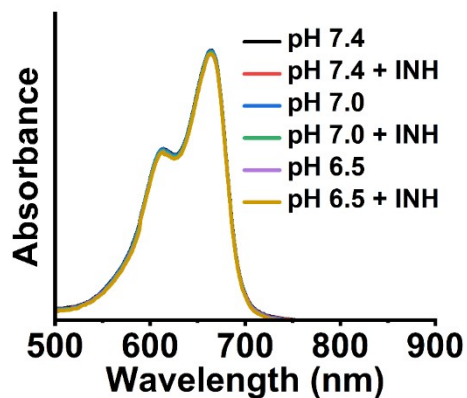


Fig. S1. UV-Vis absorption spectra of MB in the presence of INH at different pH values.

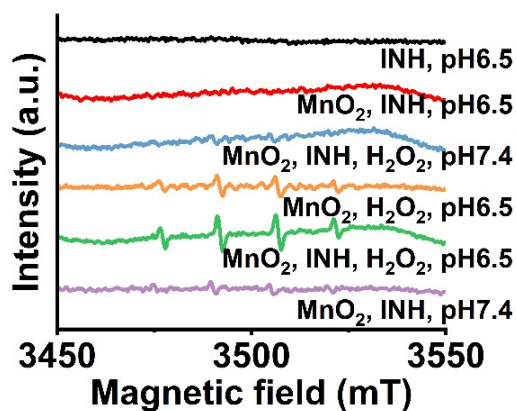


Fig. S2. ESR spectra of different solutions with DMPO (100 μM) as a spin trap.

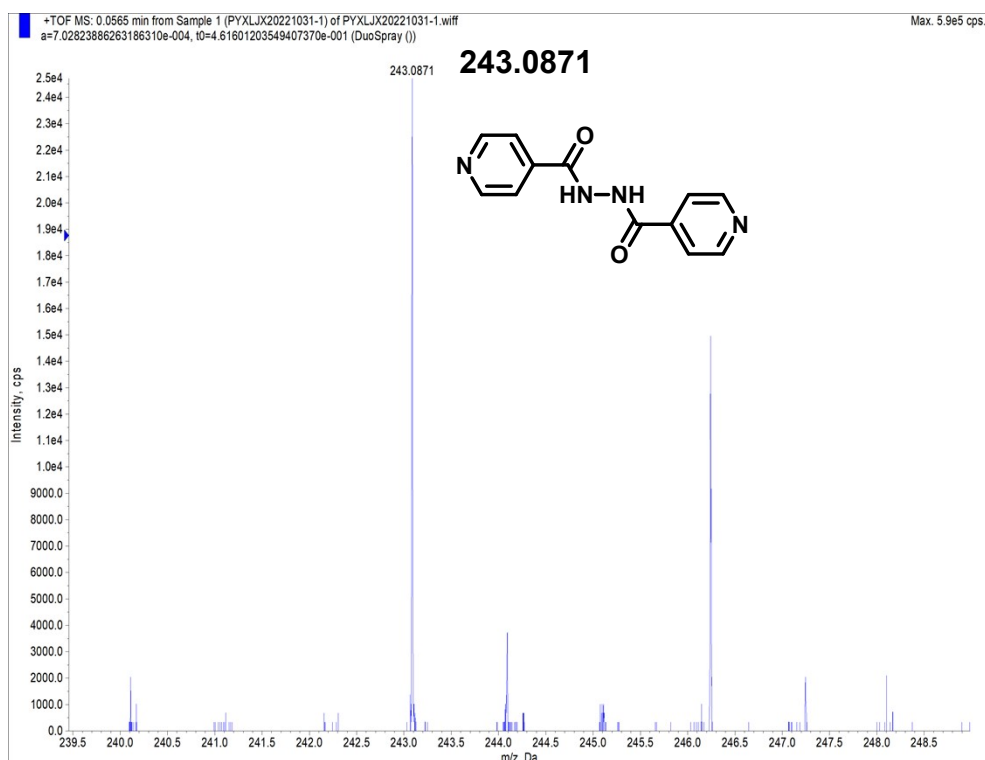
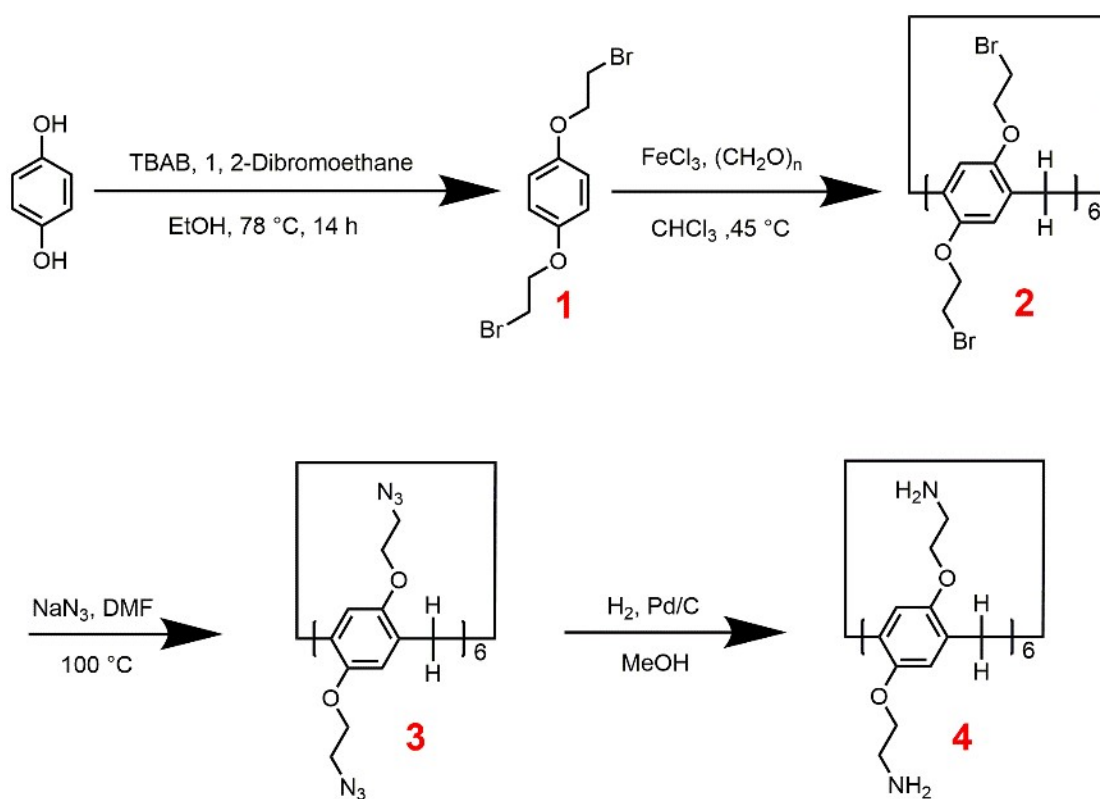


Fig. S5. The mechanism of $\cdot R$ and $\cdot OH$ generation.

Synthesis and characterizations of the compounds



Scheme S1. Synthetic route of Compound **4**.

Synthesis of Compound 1: The synthesis of Compound **1** was modified from a literature procedure³. Hydroquinone (5.0 g, 45.5 mmol), and TBAB (0.84 g, 2.4 mmol) were added into EtOH (10 mL) and the mixture were stirred at room temperature for 30 min. Then 1,2-dibromoethane (80 mL, 0.94 mol) was added and the mixture was heated to refluxed for 14 h under N₂. After that the reaction mixture was cooled down to room temperature, and precipitate was removed by filtration. The solvent was removed under reduced pressure and the product was purified by column chromatography (eluent: PE:DCM = 1:1, v:v). Compound **1** was obtained as white solid (7.510 g, 51%). ¹H NMR δ (ppm) (500 MHz, CDCl₃) 6.86 (s, 4H), 4.25 (t, *J* = 6.5 Hz, 4H), 3.61 (t, *J* = 6.15 Hz, 4H).

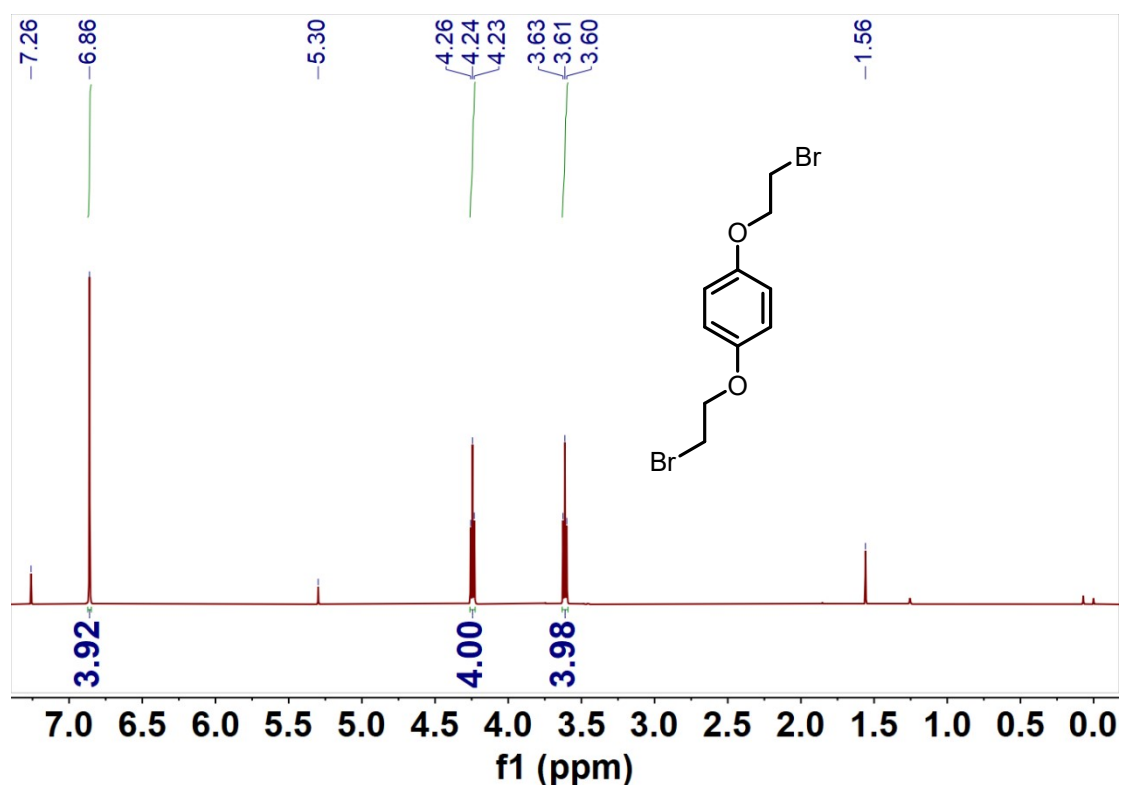


Fig. S6. The ¹H NMR (500 MHz, 298K, CDCl₃) spectrum of Compound **1**.

Synthesis of Compound 2: The synthesis of Compound 2 was modified from a literature procedure⁴. **1** (500 mg, 1.54 mmol), paraformaldehyde (232 mg, 7.71 mmol) and FeCl₃ (80 mg, 0.99 mmol) were added to CHCl₃ (23 mL), and the mixture was heated to 45 °C. The mixture was cooled down to room temperature and then washed by water for 3 times, the organic phase was concentrated and subjected to column chromatography (eluent: PE:DCM:EA = 2:1:0.06, v:v:v). Finally, Compound 2 was obtained as yellow solid (57.2 mg, 11%). ¹H NMR δ (ppm) (500 MHz, CDCl₃) 6.78 (s, 12H), 4.16 (t, *J* = 5.75 Hz, 24H), 3.87 (s, 12H), 3.55 (t, *J* = 5.75 Hz, 24H).

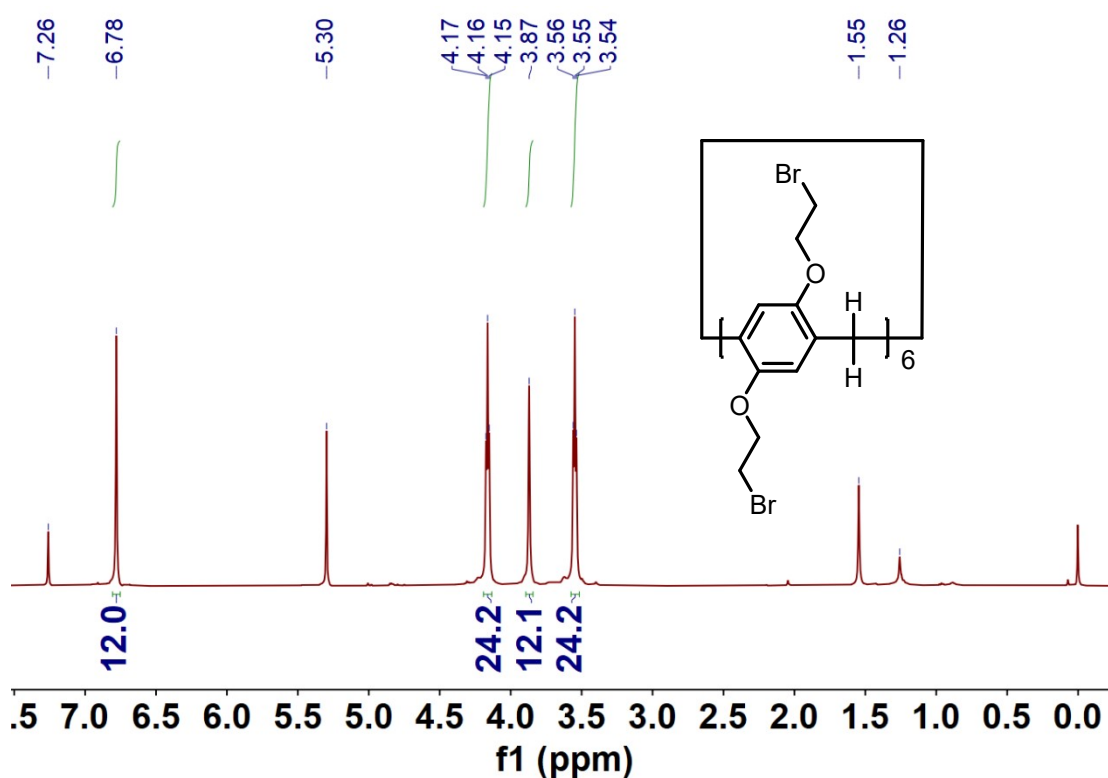


Fig. S7. The ¹H NMR (500 MHz, 298K, CDCl₃) spectrum of Compound 2.

Synthesis of Compound 3: The synthesis of Compound **3** was modified from a literature procedure⁴. To a solution of Compound **2** (220 mg, 0.09 mmol) in anhydrous DMF (3 mL) was added sodium azide (100 mg, 1.54 mmol) under argon atmosphere. After stirring at 100 °C for 12 h., the mixture was cooled to room temperature and poured into water (30 mL). The precipitate was collected by filtration, and washed with water to afford **3** as a yellow solid (156.8 mg, 92%). ¹H NMR δ (ppm) (500 MHz, CDCl₃) 6.74 (s, 12H), 3.97 (t, *J* = 5.0 Hz, 24H), 3.87 (s, 12H), 3.46 (t, *J* = 5.0 Hz, 24H).

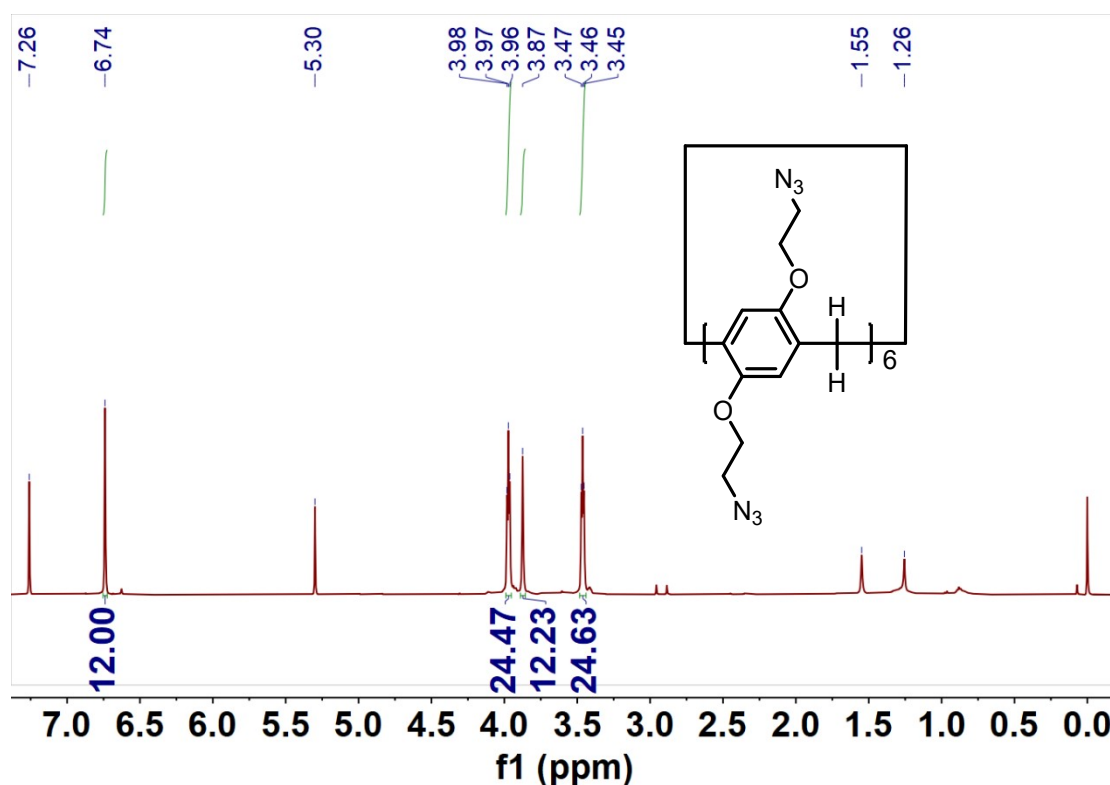


Fig. S8. The ¹H NMR (500 MHz, 298K, CDCl₃) spectrum of Compound **3**.

Synthesis of Compound 4: A suspension of **3** (40.65 mg, 0.026 mmol) and Pd/C (5%, 18 mg) in methanol was stirred at 50 °C under hydrogen atmosphere for 48 h. The resulting mixture was filtered, and the filtrate was concentrated under vacuum to afford **4** as pale-brown solid (32 mg, 98%). ^1H NMR δ (ppm) (400 MHz, D_2O) 6.81 (s, 12H), 4.07 – 4.02 (m, 24H), 3.96 (s, 12H), 3.20 (t, J = 5.1 Hz, 24H). ^{13}C NMR δ (ppm) (125 MHz, D_2O) 150.04, 129.00, 115.94, 65.41, 38.99, 29.65. HRMS (ESI-TOF) (m/z): Calcd. for $[\text{M}+\text{H}]^+$ $\text{C}_{66}\text{H}_{97}\text{N}_{12}\text{O}_{12}^+$, 1249.7344; found 1249.7330. Calcd. for $[\text{M}+2\text{H}]^{2+}$ $\text{C}_{66}\text{H}_{98}\text{N}_{12}\text{O}_{12}^{2+}$, 625.3708; found 625.3699. Calcd. for $[\text{M}+3\text{H}]^{3+}$ $\text{C}_{66}\text{H}_{99}\text{N}_{12}\text{O}_{12}^{3+}$, 417.2496; found 417.2490. Calcd. for $[\text{M}+4\text{H}]^{4+}$ $\text{C}_{66}\text{H}_{100}\text{N}_{12}\text{O}_{12}^{4+}$, 313.1891; found 313.1893.

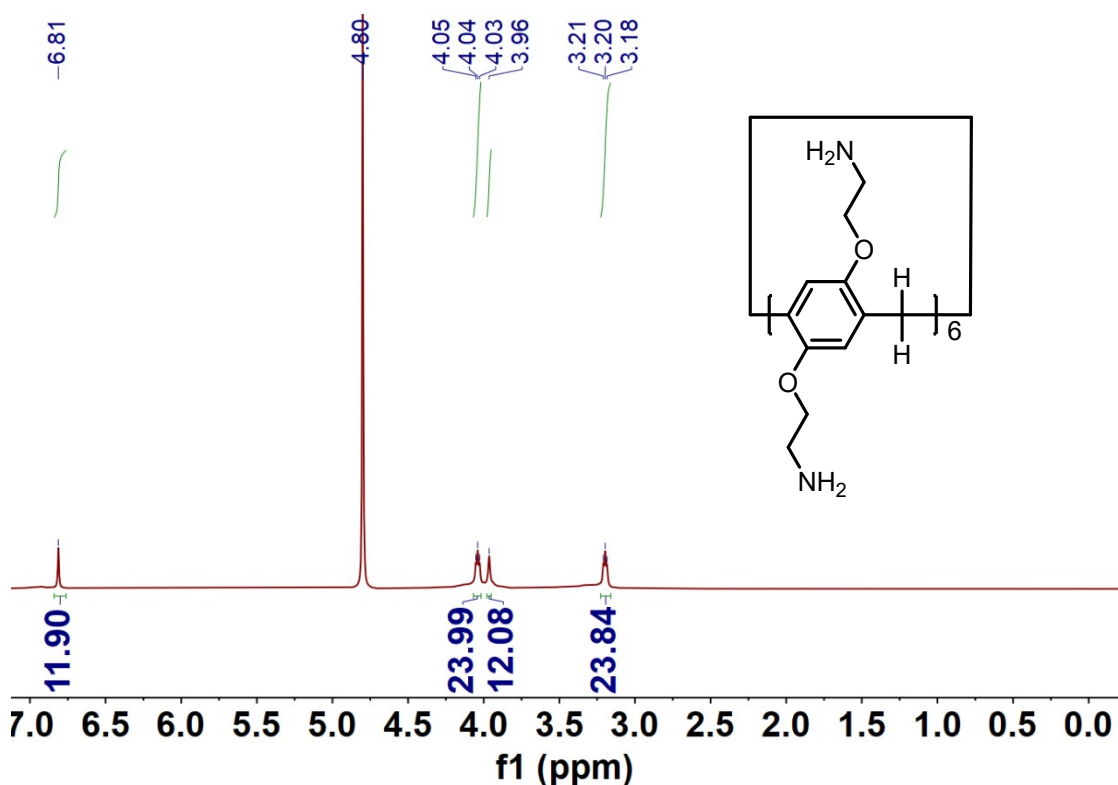


Fig. S9. The ^1H NMR (400 MHz, 298K, D_2O) spectrum of Compound 4.

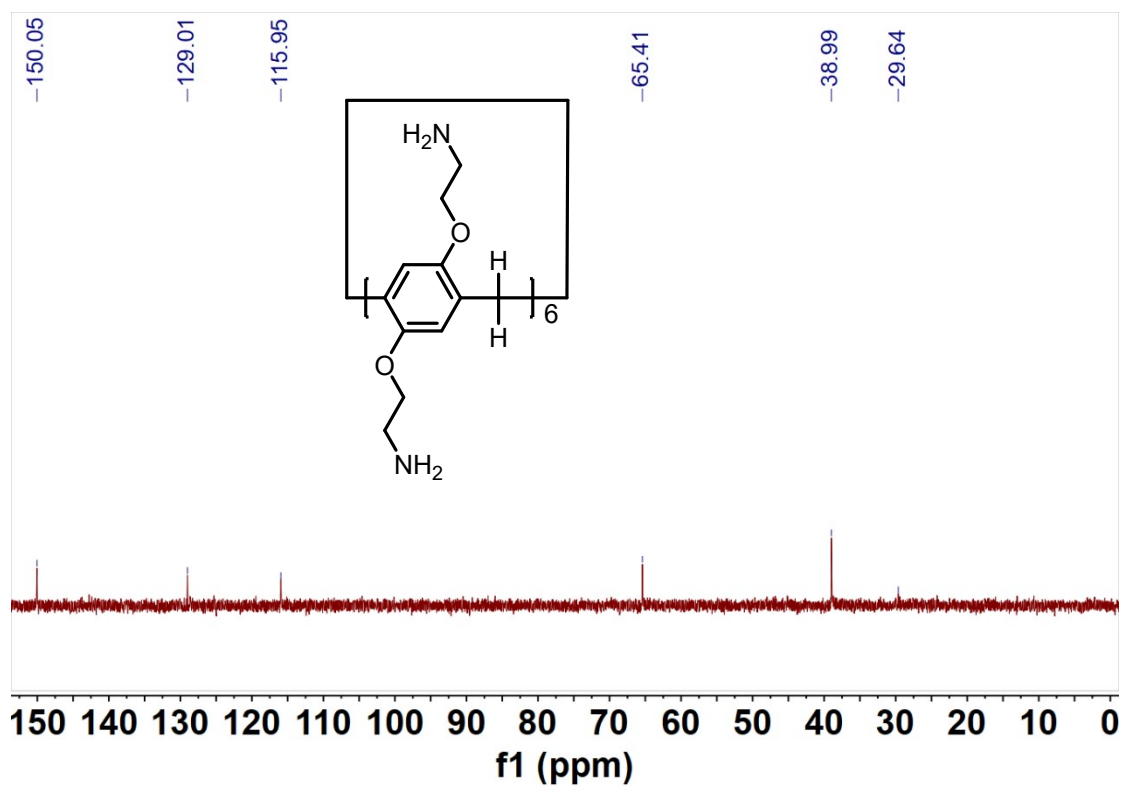


Fig. S10. The ¹³C NMR (125 MHz, 298K, D₂O) spectrum of Compound 4.

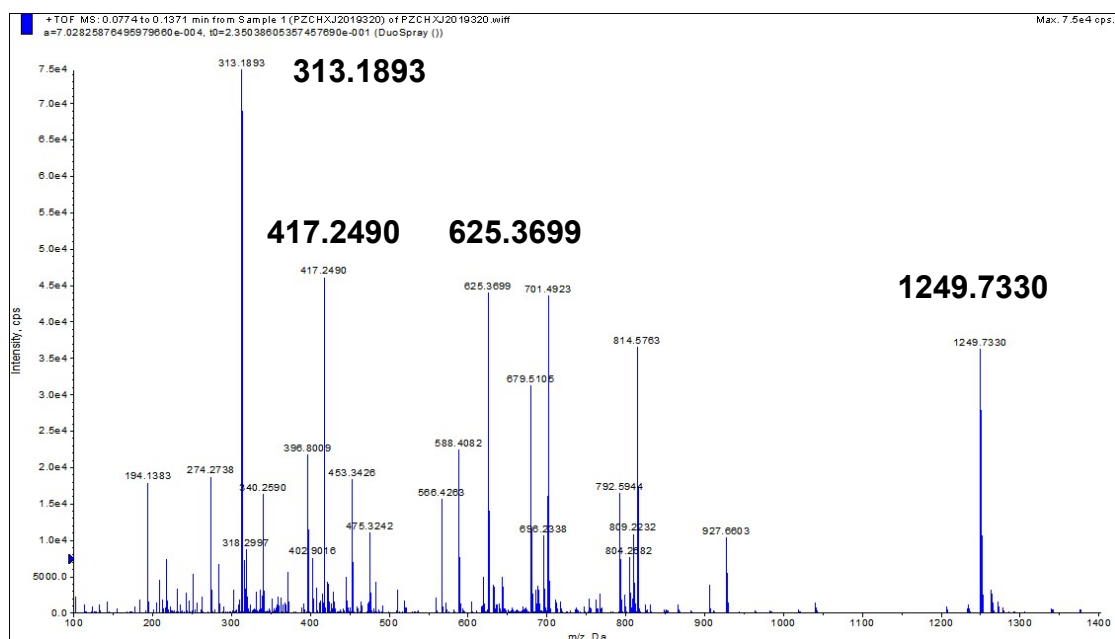
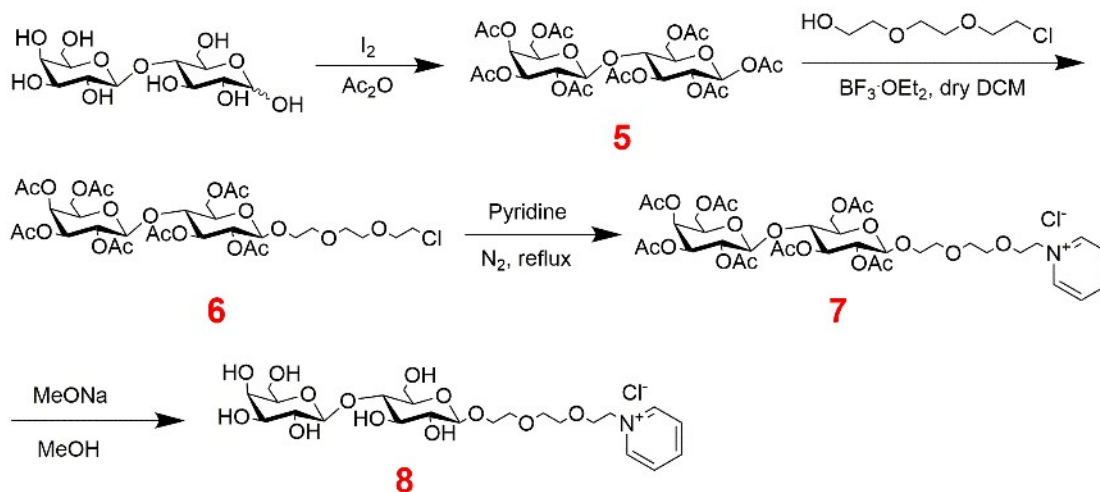


Fig. S11. HRMS spectrum of Compound 4.



Scheme S2. Synthetic route of Compound **8**.

Synthesis of Compound 5: The synthesis of Compound **5** was modified from a literature procedure⁵. D-Lactose monohydrate (4.82 g, 13.4 mmol) and iodine (0.247 g, 0.97 mmol) were mixed in acetic anhydride (30 mL). Then, the mixture was stirred at room temperature for 24 h. After the reaction completed, the mixture was diluted with dichloromethane (100 mL) and was washed against saturated Na_2CO_3 aqueous solution. The solvent was evaporated under reduced pressure to afford Compound **5** (10.7g, 99%) as white powder. ^1H NMR δ (ppm) (400 MHz, CDCl_3) 6.23 (d, $J = 3.5$ Hz, 1H), 5.44 (t, $J = 9.7$ Hz, 1H), 5.34 (d, $J = 2.9$ Hz, 1H), 5.10 (dd, $J = 10.2, 8.0$ Hz, 1H), 5.00 – 4.92 (m, 2H), 4.48 – 4.42 (m, 2H), 4.11 – 4.07 (m, 3H), 3.99 (d, $J = 10.1$ Hz, 1H), 3.87 (t, $J = 6.7$ Hz, 1H), 3.80 (t, $J = 9.7$ Hz, 1H), 2.15 (s, 3H), 2.13 (s, 3H), 2.10 (s, 3H), 2.04 (s, 3H), 2.03 (s, 3H), 2.01 (s, 3H), 1.98 (s, 3H), 1.94 (s, 3H),.

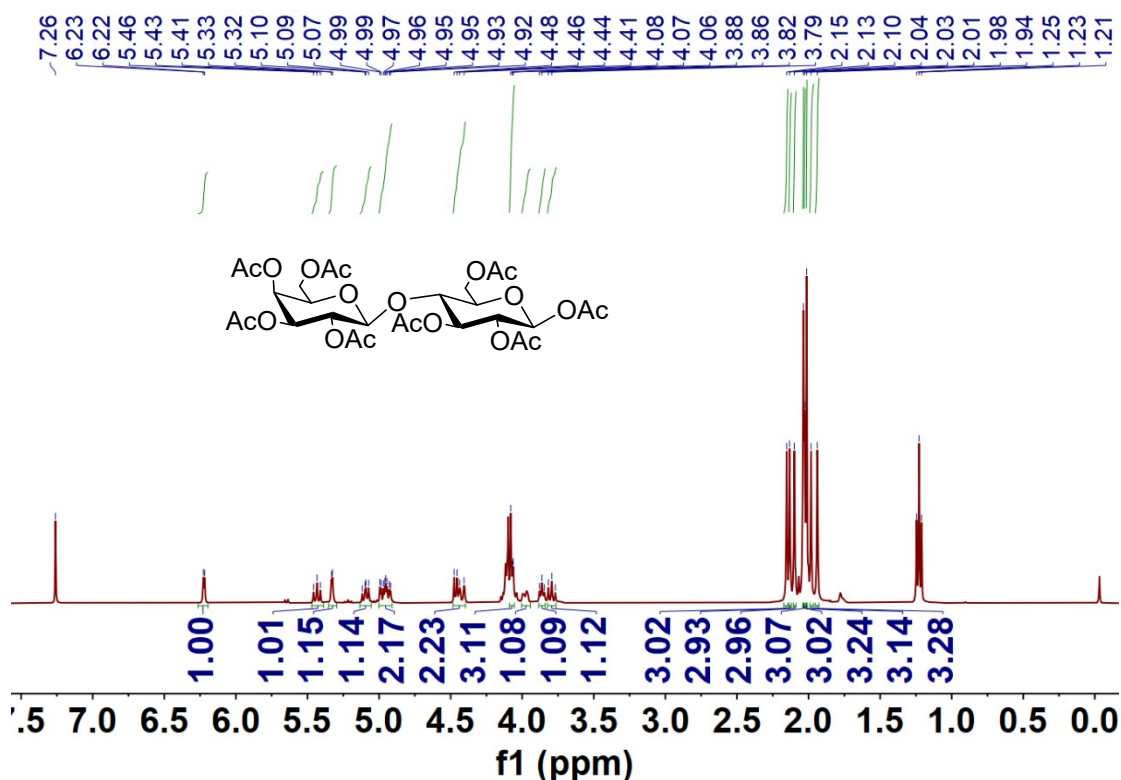


Fig. S12. The ^1H NMR (400 MHz, 298K, CDCl_3) spectrum of Compound **5**.

Synthesis of Compound 6: The synthesis of Compound **6** was modified from a literature procedure⁵. Compound **5** (1.5 g, 2.21 mmol) and 2-(2-(2-chloroethoxy) ethoxy) ethanol (1.1 g, 6.63 mmol) were dissolved in dry CH_2Cl_2 (18.4 mL) under nitrogen atmosphere. The mixture was cooled to 0 °C, and $\text{BF}_3 \cdot \text{Et}_2\text{O}$ (1 mL, 8.29 mmol) was slowly added. The reaction was stirred overnight at room temperature. After the reaction completed, the mixture was washed twice with saturated NaHCO_3 solution, the organic phase was dried over anhydrous sodium sulfate. The solvent was removed under reduced pressure. Flash column chromatography (eluent: EA:PE = 2:3 to 3:2, v:v) to afford Compound **6** (0.89 g, 1.134 mmol, 51%) as white foam. ^1H NMR δ (ppm) (500 MHz, CDCl_3) 5.35 (d, J = 2.9 Hz, 1H), 5.19 (t, J = 9.3 Hz, 1H), 5.11 (dd, J = 10.4, 7.9 Hz, 1H), 4.95 (dd, J = 10.4, 3.4 Hz, 1H), 4.90 (dd, J = 9.5, 8.0 Hz, 1H), 4.57 (d, J = 7.9 Hz, 1H), 4.51 – 4.43 (m, 2H), 4.16 – 4.04 (m, 4H), 3.93 – 3.86 (m, 2H), 3.81 – 3.72 (m, 4H), 3.68 – 3.59 (m, 9H), 2.15 (s, 3H), 2.12 (s, 3H), 2.06 (s, 3H), 2.06 – 2.04 (m, 9H), 1.97 (s, 3H).

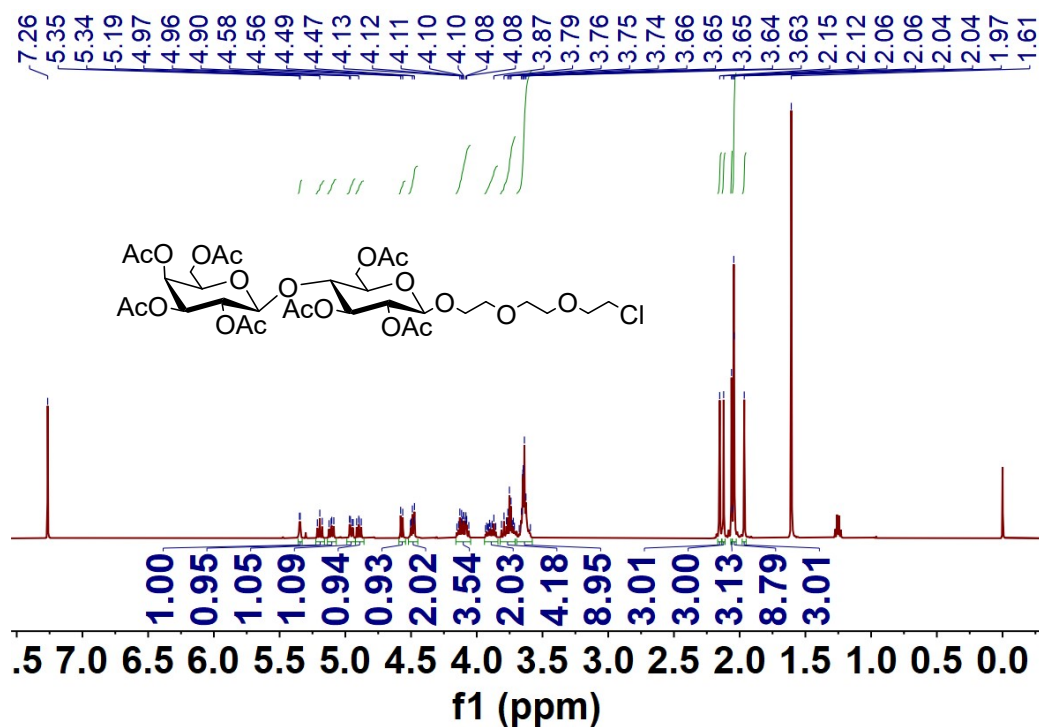


Fig. S13. The ^1H NMR (500 MHz, 298K, CDCl_3) spectrum of Compound **6**.

The synthesis of Compound 7: The synthesis of Compound **7** was modified from a literature procedure⁶. The Compound **6** (207 mg, 0.263 mmol) was dissolved in 8 mL pyridine. The mixture was reflux under nitrogen atmosphere for 12 h, then concentrated under reduced pressure. The crude product was purified by flash column chromatography (eluent: PE:EA = 1:3) to give Compound **7** as a yellow oil (125 mg, 55 %). ^1H NMR δ (ppm) (400 MHz, CD_3OH) 9.00 (d, $J = 6.0$ Hz, 2H), 8.63 (t, $J = 8.1$ Hz, 1H), 8.13 (t, $J = 6.7$ Hz, 2H), 5.35 (s, 1H), 5.14 (dd, $J = 26.1, 9.9$ Hz, 2H), 5.04 – 4.95 (m, 1H), 4.73 – 4.64 (m, 2H), 4.51 (d, $J = 12.0$ Hz, 1H), 4.18 (dd, $J = 12.2, 5.4$ Hz, 1H), 4.12 (s, 3H), 3.99 (s, 2H), 3.85 (t, $J = 9.0$ Hz, 2H), 3.78 – 3.65 (m, 2H), 3.61 (s, 2H), 3.54 (s, 4H), 3.30 (s, 3H), 2.12 (s, 3H), 2.10 (s, 3H), 2.05 – 2.03 (m, 9H), 2.00 (s, 3H), 1.91 (s, 3H). ^{13}C NMR δ (ppm) (125 MHz, CDCl_3) 170.68, 170.64, 170.42, 170.30, 170.05, 170.02, 169.46, 146.28, 145.70, 142.87, 128.40, 128.27, 101.23, 101.10, 76.48, 73.23, 72.99, 71.83, 71.27, 70.88, 70.71, 70.50, 70.42, 69.81, 69.71, 69.42, 66.97, 62.31, 61.54, 61.02, 21.29, 21.24, 21.14, 21.12, 20.98, 20.96, 20.83. HRMS (ESI-TOF) (m/z): Calcd. for $[\text{M}-\text{Cl}]^+$ $\text{C}_{37}\text{H}_{52}\text{NO}_{20}^+$, 830.3078, found 830.3078.

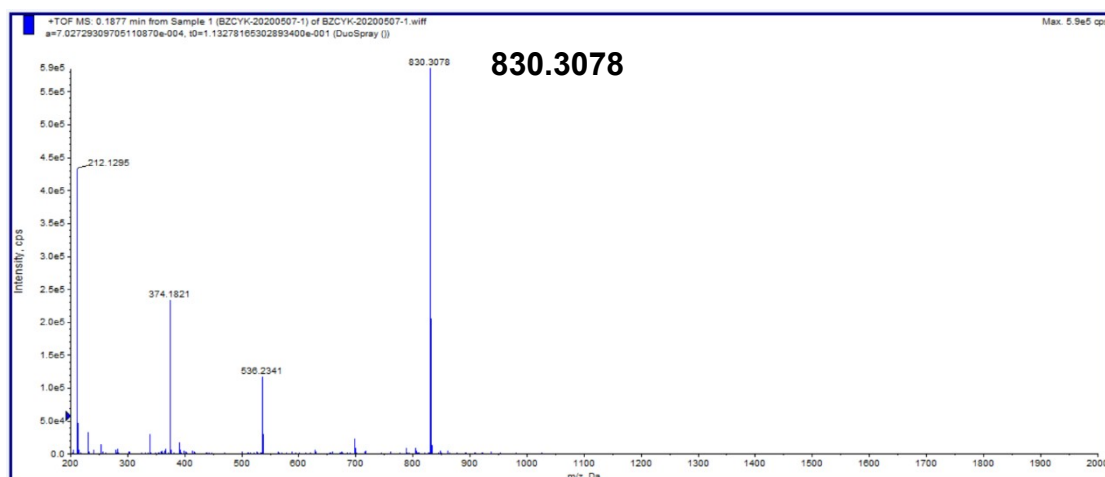


Fig. S16. HRMS spectrum of Compound 7.

The synthesis of Compound 8: The synthesis of Compound 8 was modified from a literature procedure⁶. MeONa (108 mg, 2 mmol) was added into a solution of Compound 7 (173 mg, 0.2 mmol in 10 mL MeOH). The mixture was stirred at room temperature for 4 h, then neutralized by addition of ion-exchange resin (Amberlite IR 120 H⁺) until pH 7, filtered, and the solvent was removed under reduced pressure. The 8 was obtained as a yellow oil (103 mg, 92 %). ¹H NMR δ (ppm) (500 MHz, D₂O) 8.88 (d, *J* = 6.0 Hz, 2H), 8.59 (t, *J* = 8.0 Hz, 1H), 8.09 (t, *J* = 7.0 Hz, 2H), 4.51 (d, *J* = 8.0 Hz, 1H), 4.45 (d, *J* = 7.8 Hz, 1H), 4.04 (t, *J* = 5.0 Hz, 2H), 4.01 – 3.97 (m, 1H), 3.93 (d, *J* = 3.0 Hz, 1H), 3.84 – 3.71 (m, 7H), 3.68 – 3.64 (m, 10H), 3.61 – 3.59 (m, 1H), 3.56 – 3.52 (m, 2H). ¹³C NMR δ (ppm) (125 MHz, D₂O) 146.03, 144.76, 128.08, 102.94, 102.07, 78.39, 75.37, 74.76, 74.34, 72.83, 72.52, 70.96, 69.75, 69.63, 69.45, 68.73, 68.71, 68.57, 61.05, 60.08, 48.93. HRMS (m/z): Calcd. for [M-Cl]⁺ C₂₃H₃₈NO₁₃⁺, 536.2338, found 536.2315.

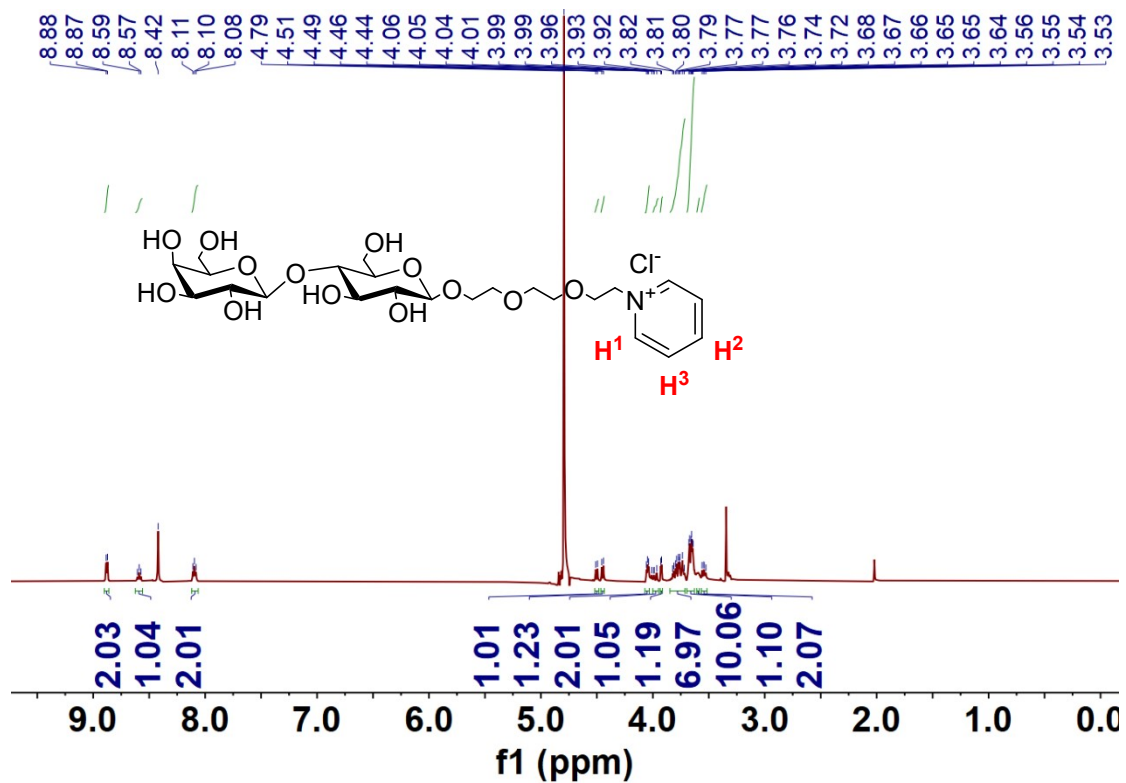


Fig. S17. The ^1H NMR (500 MHz, 298K, D_2O) spectrum of Compound 8.

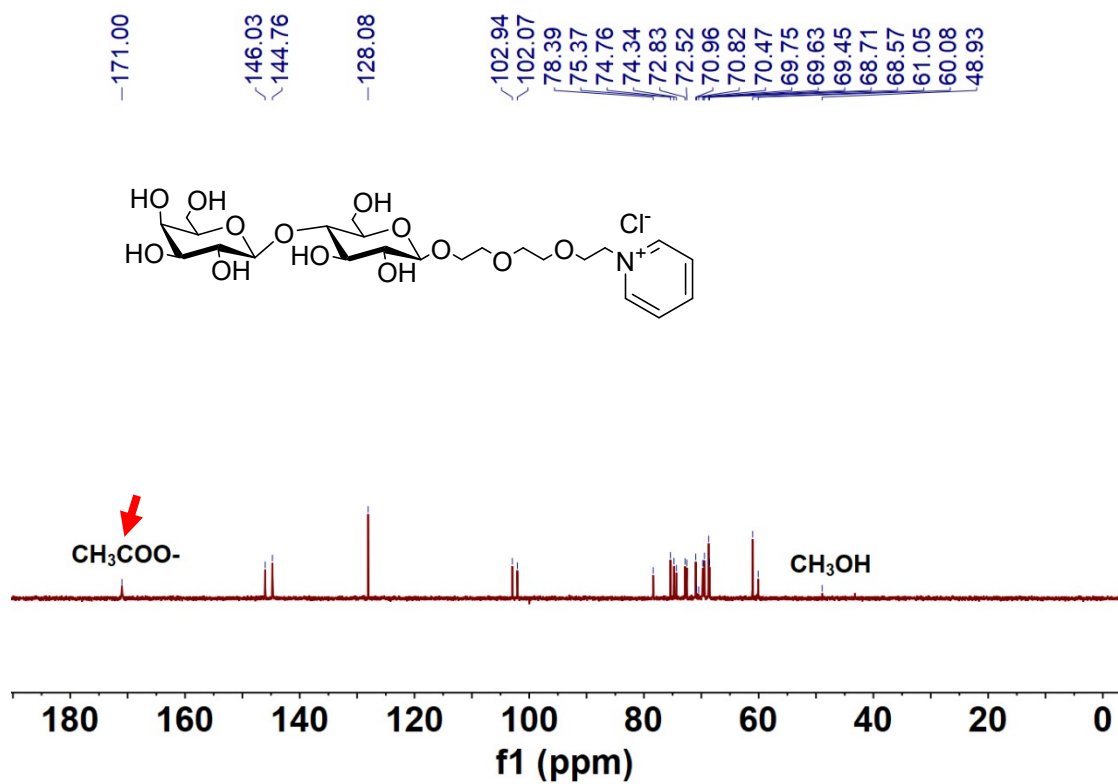


Fig. S18. The ^{13}C NMR (125 MHz, 298K, D_2O) spectrum of Compound 8.

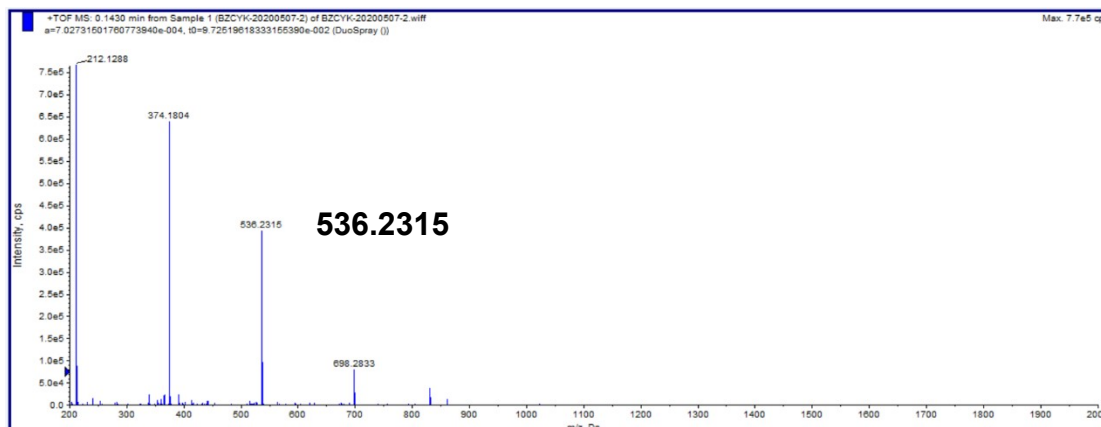
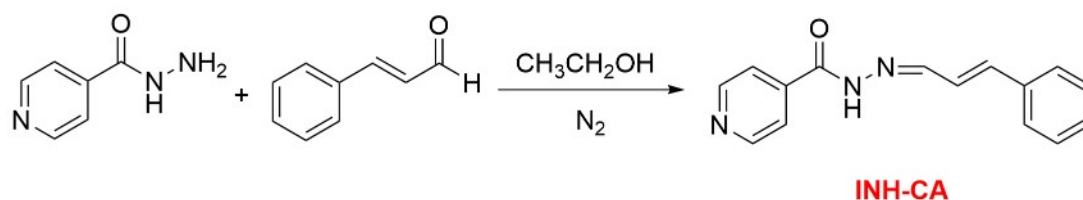


Fig. S19. HRMS spectrum of Compound **8**.



Scheme S3. Synthetic route of compound INH-CA

The synthesis of compound INH-CA: Add isoniazid (274.4 mg, 2 mmol) to a 10 mL flask. Under anhydrous and nitrogen protection, ethanol (3 mL) and cinnamaldehyde (317.2 mg) were added. The mixture was stirred at room temperature until a milky yellow precipitate formed. The product was collected by filtration, washed with petroleum ether and RO water. INH-CA (260.1 mg, 52%) is obtained by vacuum drying. ^1H NMR δ (ppm) (400 MHz, DMSO- d_6) 11.97 (s, 1H), 8.78 (dd, $J = 6.1$ Hz, 2.3 Hz, 2H), 8.24 (dd, $J = 6.1$, 2.3 Hz, 1H), 7.80 (d, $J = 6.0$ Hz, 2H), 7.64 (d, $J = 7.1$ Hz, 2H), 7.40 (t, $J = 7.2$ Hz, 2H), 7.34 (d, $J = 6.9$ Hz, 1H), 7.11 (s, 1H), 7.09 (d, $J = 6.3$ Hz, 1H). ^{13}C NMR δ (ppm) (100 MHz, D_2O) 161.93, 151.54, 150.79, 140.93, 140.39, 136.27, 129.50, 129.33, 127.69, 125.87, 122.00. HRMS (m/z): Calcd. for $[\text{M}+\text{H}]^+$ $\text{C}_{15}\text{H}_{14}\text{N}_3\text{O}^+$, 252.1131, found 252.1137.

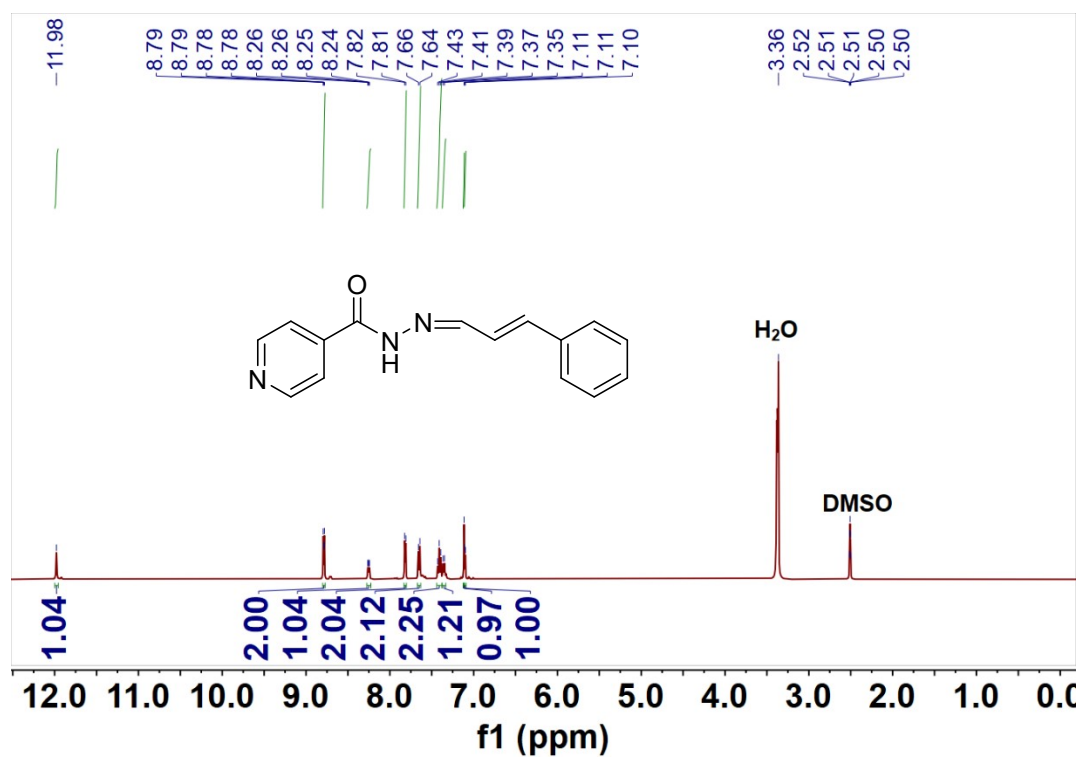


Fig. S20. The ^1H NMR (400 MHz, 298K, DMSO) spectrum of compound INH-CA.

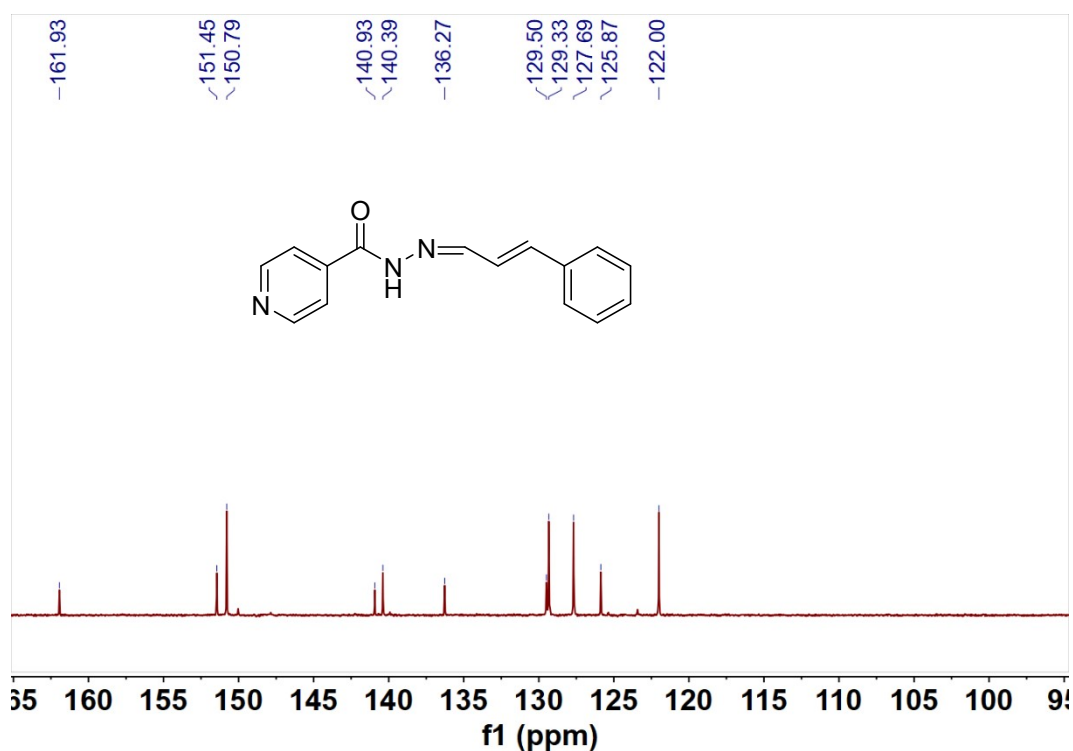


Fig. S21. The ^{13}C NMR (100 MHz, 298K, DMSO) spectrum of compound INH-CA.

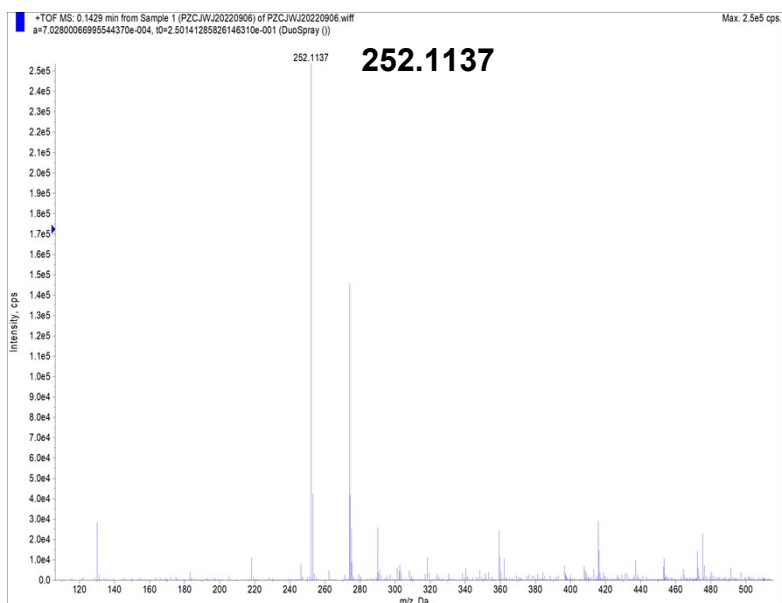


Fig. S22. HRMS spectrum of compound INH-CA.

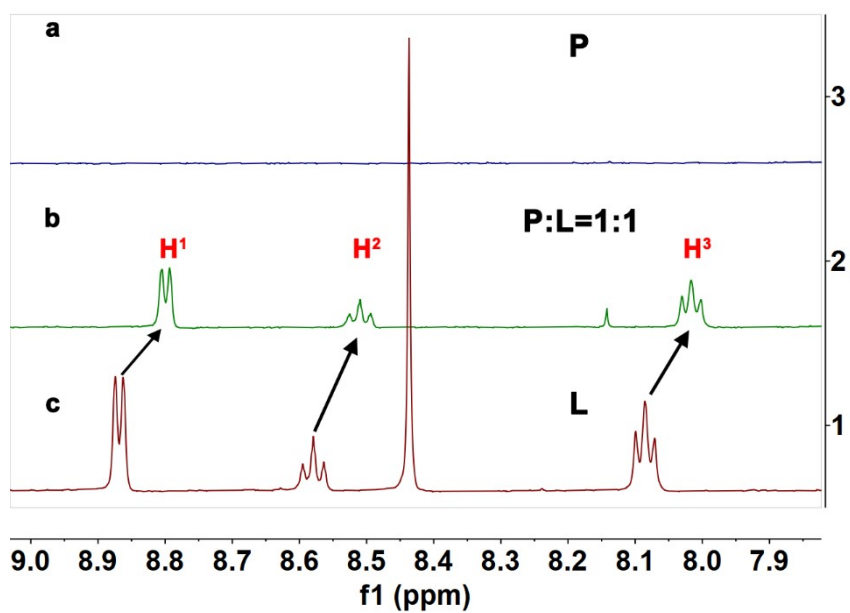


Fig. S23. ^1H NMR spectra (500 MHz, D_2O , 298 K): (a) amino pillar[6]arene (P) (10 mM); (b) P:L = 1:1; (c) Lactose-pyridine (L) (10 mM). (H^1 , H^2 , and H^3 are defined in Figure S16)

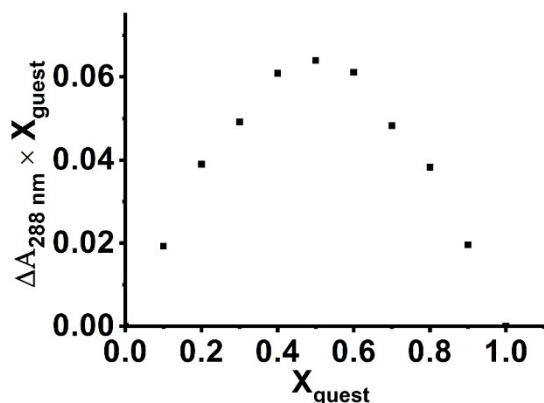


Fig. S24. The binding stoichiometry of amino pillar[6]arene (**P**) and Lactose-pyridine (**L**).

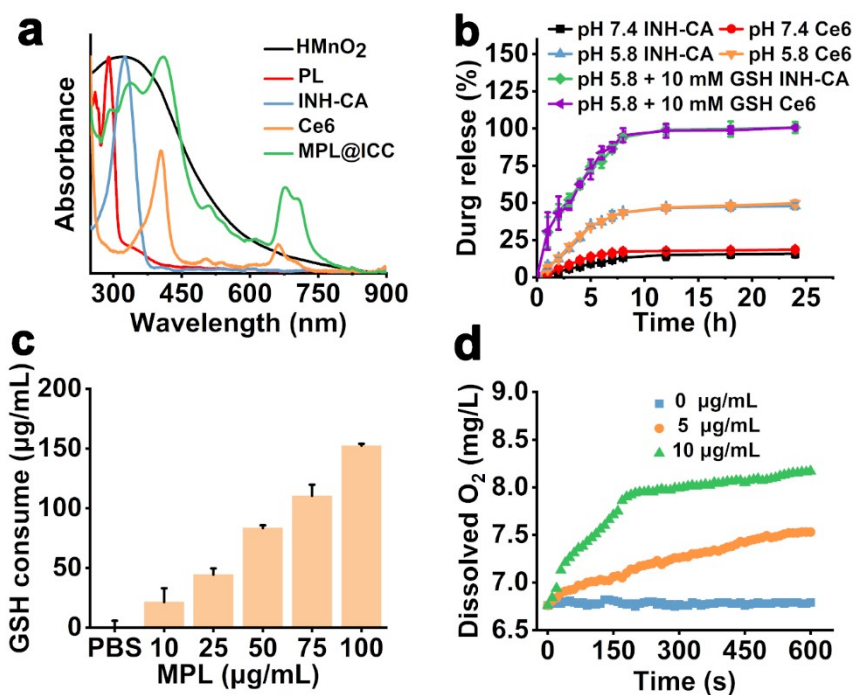


Fig. S25. (a) UV-vis spectra of free Ce6, INH-CA, PL, HMnO₂, and MPL@ICC. (b) Percentages of released Ce6 and INH-CA from MPL@ICC over time at different conditions (pH 7.4, 5.8 and with/without 10 mM GSH). ($n = 3$) (c) The GSH consume after various concentrations of MPL were added. ($n = 3$) (d) The O₂ concentration changes in H₂O₂ solutions (100 μM) after various concentrations of HMnO₂ were added.

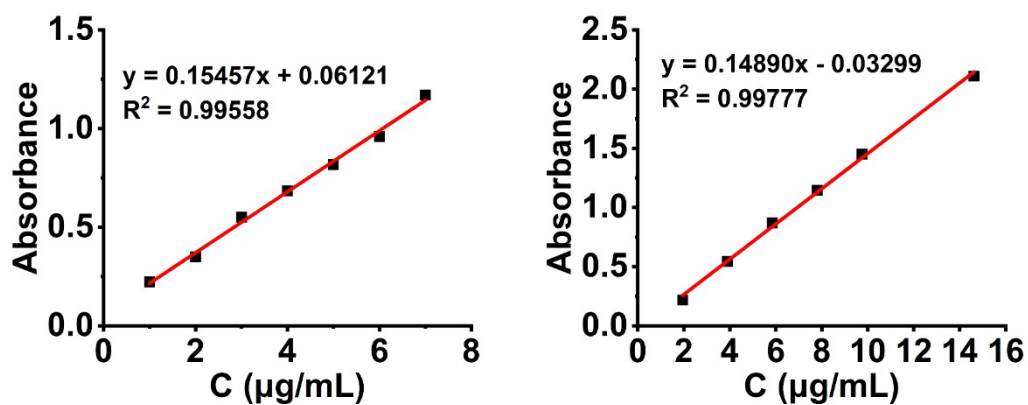


Fig. S26. The standard curve of Ce6 (left) and the standard curve of IHN-CA (right).

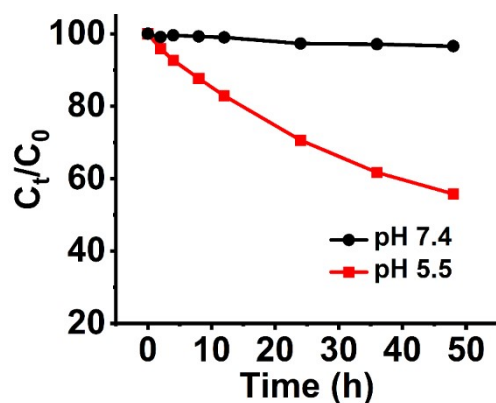


Fig. S27. Degradation curves of IHN-CA at pH 7.4 and pH 5.5 under 37 °C.

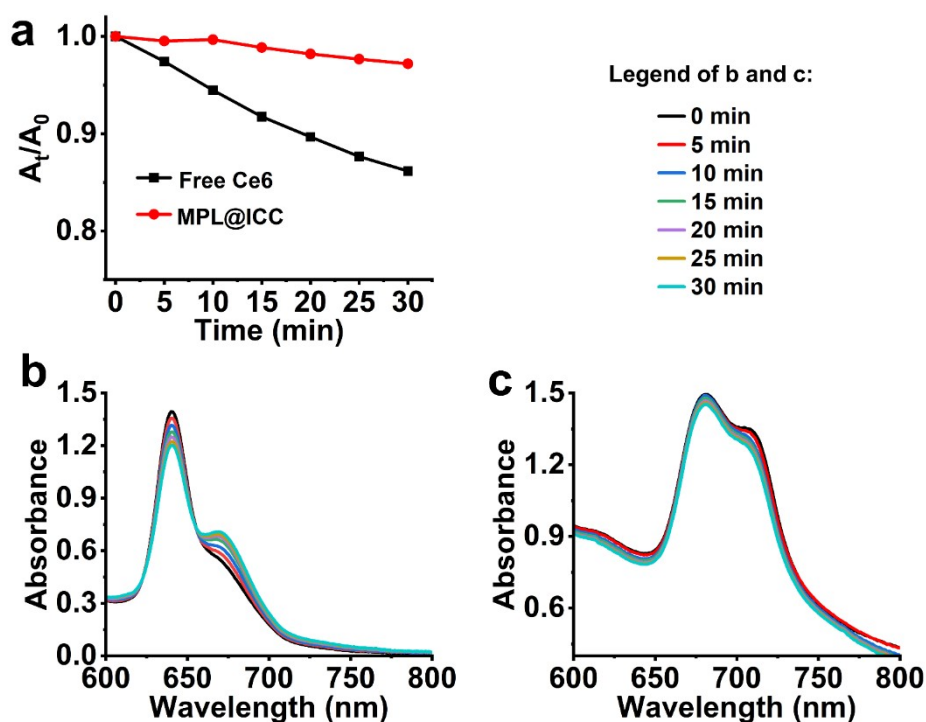


Fig. S28. The Photostability of free Ce6 and MPL@ICC (660 nm, 7 mW/cm²). (a) A_t/A_0 of free Ce6 and MPL@ICC with different irradiation time. (b) The UV-Vis absorption spectra of free Ce6 with different time irradiation. (c) The UV-Vis absorption spectra of MPL@ICC with different irradiation time.

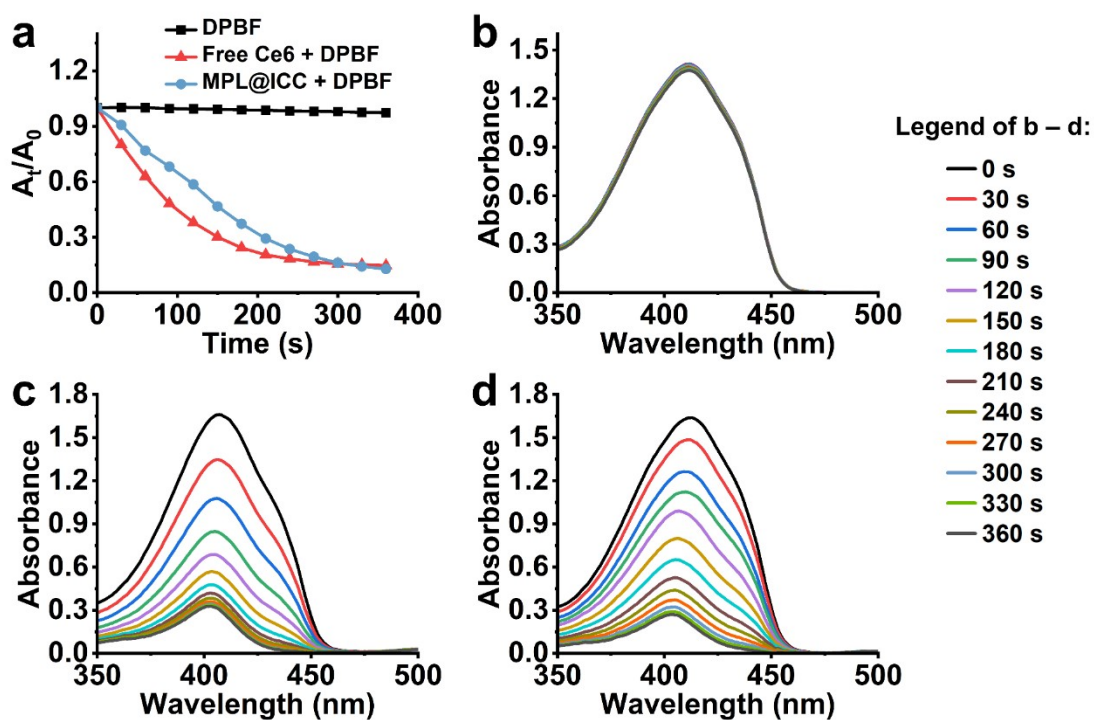


Fig. S29. The ¹O₂ generated by free Ce6 and MPL@ICC under 660 nm laser

irradiation (5 mW/cm²). (a) A_i/A_0 of DPBF at 412 nm in different solutions with different irradiation time. (b) The UV-Vis absorption spectra of DPBF with different irradiation time. (c) The UV-Vis absorption spectra of free Ce6 + DPBF with different irradiation time. (d) The UV-Vis absorption spectra of MPL@ICC + DPBF with different irradiation time.

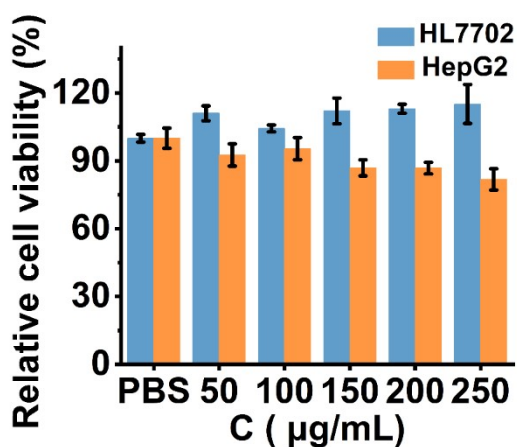


Fig. S30. The relative cell viabilities of HL7702 cells and HepG2 cells after incubation with MPL for 24 h at various doses ($n = 5$, 5×10^3 cells per well)

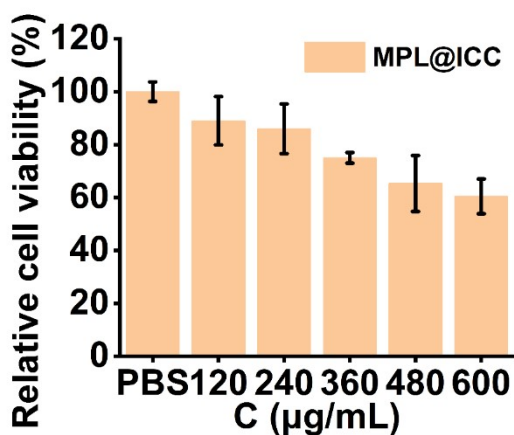


Fig. S31. Relative cell viability of HL7702 cells incubated with MPL@ICC for 24h. Data are expressed as means \pm SD ($n = 5$).

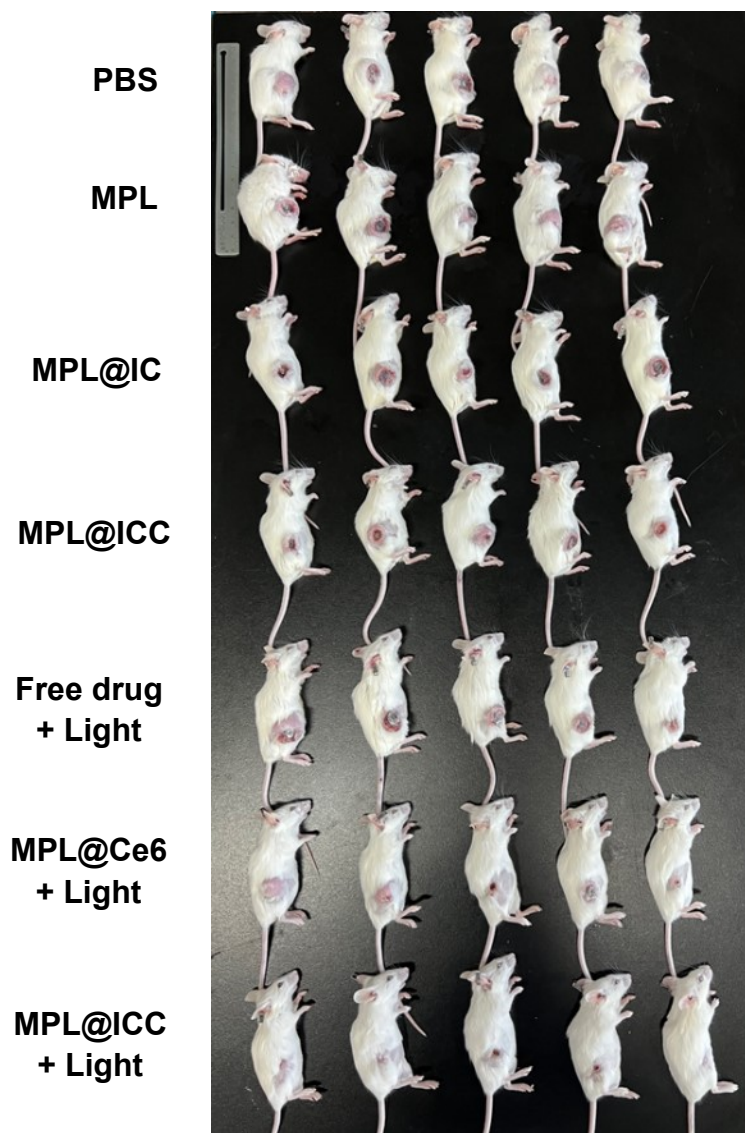


Fig. S32. Photo of the mice at the end of the treatment.

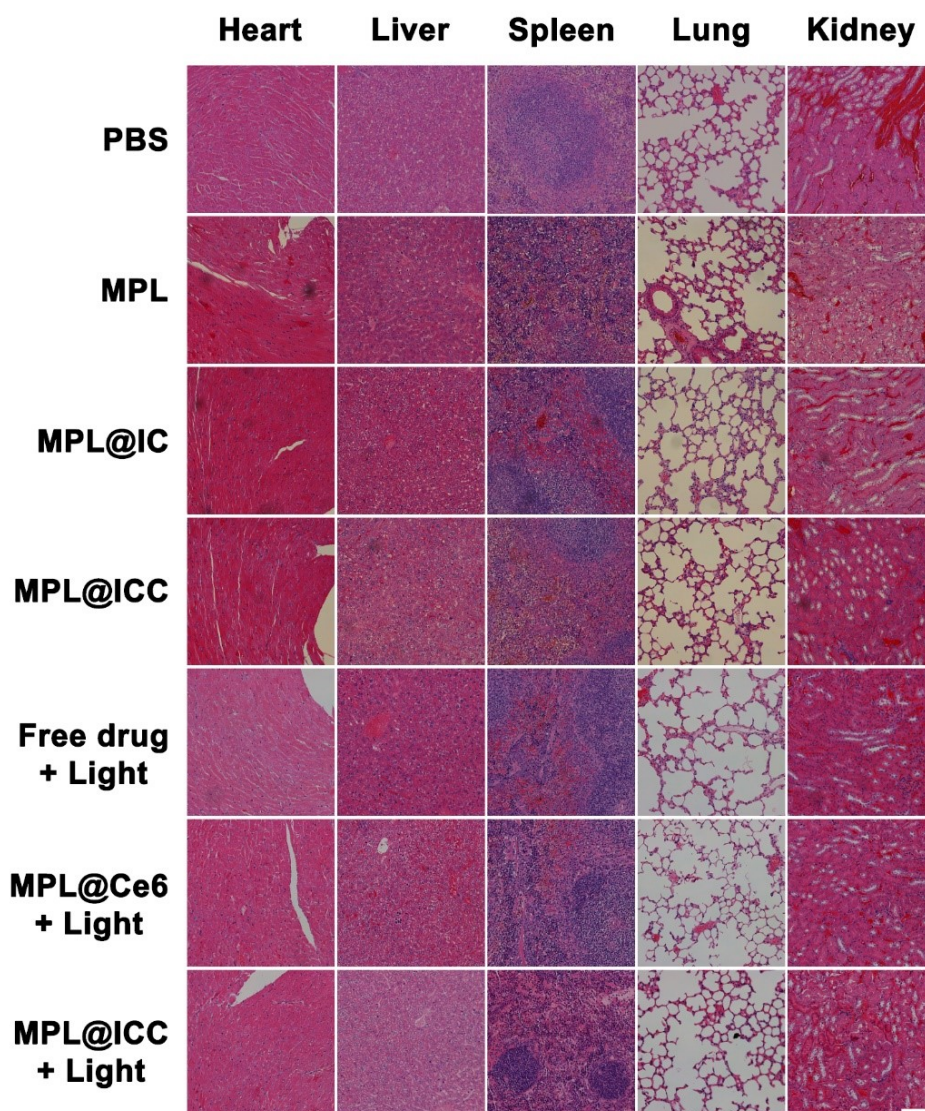


Fig. S33. H&E staining of mouse major organs. Scale bar: 100 μ m.

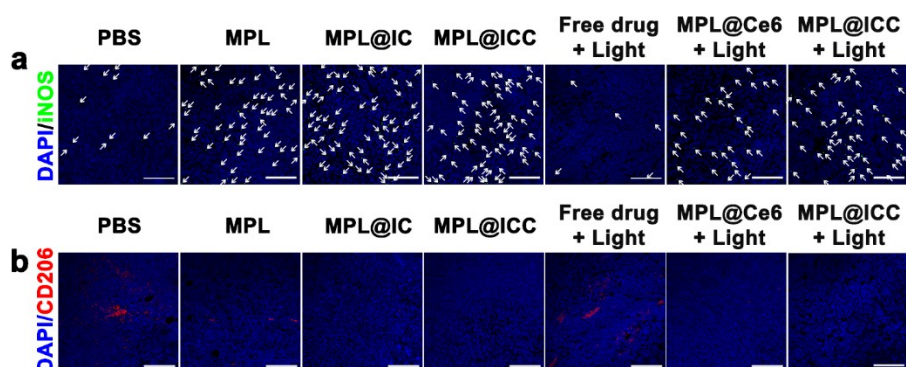


Fig. S34. Representative fluorescent images of (a) M1 and (b) M2 macrophage in tumors. Scale bar: 100 μ m. The percentage statistics of M1 and M2 macrophages are shown in Fig. 8e.

References:

1. H. E. Gottlieb, V. Kotlyar, A. Nudelman, *J. Org. Chem.* **1997**, *62*, 7512-7515.
2. L. Qin, C. H. Huang, D. Xu, L. N. Xie, J. Shao, L. Mao, B. Kalyanaraman, B. Z. Zhu, *Free Radical Biol. Med.* **2019**, *143*, 232-239.
3. Q. X. Liu, Z. Q. Yao, X. J. Zhao, A. H. Chen, X. Q. Yang, S. W. Liu, and X. G. Wang, *Organometallics*, **2011**, *30*, 3732-3739.
4. Q. Duan, W. Zhao, K. Lu, *Tetrahedron Lett.* **2017**, *58*, 4403-4406.
5. Q. Xiao, A. K. Ludwig, C. Romanò, I. Buzzacchera, S. E. Sherman, M. Vetro, S. Vértesy, H. Kaltner, E. H. Reed, M. Möller, C. J. Wilson, D. A. Hammer, S. Oscarson, M. L. Klein, H. J. Gabius, and V. Percec, *Proc. Natl. Acad. Sci. U. S. A.* **2018**, *115*, 201720055.
6. K. Yang, Y. C. Chang, J. Wen, Y. C. Lu, Y. X. Pei, S. P. Cao, F. Wang, and Z. C. Pei, *Chem. Mater.* **2016**, *28*, 1990-1993.